Electrochimica Acta 100 (2013) 18–23

Contents lists available at SciVerse ScienceDirect

Electrochimica Acta

journal homepage: www.elsevier.com/locate/electacta

The development of an all copper hybrid redox flow battery using deep eutectic solvents

David Lloyd*, Tuomas Vainikka, Kyösti Kontturi

Aalto University, Department of Chemistry, Kemistintie 1, PO Box 16100, 00076 Aalto, Finland

ARTICLE INFO

Article history:
Received 28 November 2012
Received in revised form 21 March 2013
Accepted 23 March 2013
Available online 31 March 2013

Keywords:
Redox flow battery
Ionic liquid
Deep eutectic solvent
All copper
Chlorocuprate

ABSTRACT

The performance of a redox flow battery based on chlorocuprates dissolved in an ionic liquid analogue is reported at 50 °C. The kinetics of the positive electrode reaction at a graphite electrode are favourable with a heterogeneous rate constant, k^0, of 9.5×10^{-4} cm s^{-1}. Coulombic efficiency was typically 94% and independent of current density. The small cell potential of 0.75 V and slow mass transport result in energy efficiencies of only 52% and 62% at current densities of 10 and 7.5 mA/cm^2 respectively. The successful development of a separator by jellifying the electrolyte using polyvinyl alcohol is reported.

1. Introduction

Redox flow batteries (RFBs) are undergoing significant research for large scale stationary energy storage applications. A typical RFB has two heterogeneous redox reactions occurring at a positive and negative electrode respectively [1]. RFBs employing the deposition/stripping reaction of a metal are known as hybrid redox flow batteries.

The RFB chemistry of greatest commercial significance is based on the multiple redox states exhibited by vanadium. However, as recently highlighted by Wadia et al. [2], there are fundamental limitations to the availability of some transition metals used in numerous RFB systems currently undergoing research, for instance vanadium and cerium [3]. For this reason, it is logical to develop simple, cost effective systems using materials exhibiting fewer supply constraints, for instance base metals and bulk chemicals.

Some ionic liquids (ILs) can be based on widely available material streams. ILs are defined as highly dissociated molten salts that are liquid below 100 °C [4]. ILs offer the scope to achieve significant increases in energy density. Firstly, they can be engineered to have extremely wide windows of electrochemical stability. This allows, for instance, the deposition of metallic lithium [5], hence large cell potentials are possible. Secondly, an electroactive species may actually be part of the ionic liquid. For instance, in ILs based on transition-metal ethanolamine cation complexes and discrete organic anions concentrations of the electroactive species of up to 6.5 M can be achieved [6].

Major challenges to the development of IL based RFB systems are their high cost and limited availability at even the tonne scale. Compared to aqueous systems they are also viscous and resistive [7]. Additionally, the preparation of a transition-metal-salt solution may require a complicated metathesis of the desired metal salt from the protonated anion [8].

Work has begun on the development of RFBs that utilise ILs [9]. Additionally, papers describing the application of ILs as supporting electrolytes in molecular solvents used in RFBs also exist [10]. To achieve a liquid state at room temperature, ILs typically require relatively bulky cations and anions, making them average supporting electrolytes when dissolved in molecular solvents compared to a typical choice, such as an alkali-metal perchlorate [11].

Deep eutectic solvents (DES) are formed when an organic halide salt, typically choline chloride, is combined with a material capable of forming a complex with the halide, such as urea, to form a material that is liquid at ambient conditions [12]. DES exhibit similar properties to chloride rich chloroaluminate ionic liquids, but can be prepared and used under ambient conditions [13]. They are often non-toxic and tend to be an order of magnitude cheaper than ionic liquids. To the best of our knowledge the use of DES as electrolyte media in a RFB has not yet been reported.

Abbott et al. were the first to report the electrochemistry of copper complexes in a DES [12]. We have recently expanded this work and found that copper can exist in three different stable states:

* Corresponding author. Tel.: +358 4578402492.
E-mail address: david.lloyd@aalto.fi (D. Lloyd).

0013-4686/$ – see front matter © 2013 Elsevier Ltd. All rights reserved.
http://dx.doi.org/10.1016/j.electacta.2013.03.130

Cu(s), $Cu(I)Cl_3^{2-}$ and $Cu(II)Cl_4^{2-}$ [14]. These states are connected by the redox reactions shown in Eqs. (1) and (2).

$$\text{Negative electrode: } CuCl_3^{2-} + e^- \underset{\text{discharge}}{\overset{\text{charge}}{\rightleftharpoons}} Cu(S) + 3Cl^- \quad (1)$$

$$\text{Positive electrode: } CuCl_4^{2-} + e^- \underset{\text{charge}}{\overset{\text{discharge}}{\rightleftharpoons}} CuCl_3^{2-} + Cl^- \quad (2)$$

The DES used in both that work and here is a mixture of choline chloride and ethylene glycol, combined in a 1:2 molar ratio, which is known as ethaline. Ethaline has the lowest viscosity and highest conductivity of this class of materials and has been studied by a number of groups for over five years [15–17].

Since ethylene glycol is a liquid at ambient conditions and no studies detailing the liquid–solid phase transition for this DES have been published, there is some ambiguity as to whether the stoichiometry commonly used corresponds to a eutectic composition. Additionally, at higher copper chloride concentrations the solute significantly competes with ethylene glycol in the complexation of chloride. At this point the system can become a ternary eutectic. For this reason in this paper we examine the reproducibility of the experimental results across a range of solute concentrations.

In ethaline the reaction shown in Eq. (2) is relatively facile at a platinum electrode with a k^0 of 10^{-3} cm s^{-1} at 25 °C and a charge transfer coefficient, α, of 0.39. With a formal potential, $E^{0\prime}$, of 0.43 V versus a Ag/AgCl reference electrode it is separated from the upper window of stability of the electrolyte by around 0.5 V. It is separated from the reaction shown in 1, for which the kinetics have not yet been characterised, by around 0.7 V [18]. This results in the two redox reactions being located centrally within the electrolytes' window of stability, which should ensure simple operation and good Coulombic efficiency if employed in an RFB.

The existence of three stable states theoretically allows the development of an all copper RFB. This was already suggested, in the form of a secondary battery, by Porterfield and Yoke for the chlorocuprate ionic liquids they investigated in the seventies [19]. Their system required the use of a protective atmosphere, exhibited a plethora of cuprate anions with various irreversible redox reactions, short circuiting due to dendrite formation and poor solubility of the Cu(II) species formed. In this work we present the first application of DES as electrolyte media for the development of what is, to the best of our knowledge, the first all-copper RFB.

Preliminary testing with commercially available separator materials has not been successful, as they show a rapid decrease in conductivity on contact with the DES. This may be due to dehydration of the membrane by the hygroscopic ionic liquid. Hence in this work we also report the development of jellified deep eutectic solvents. Jellification of ionic liquids using a polymer to form a rubbery solid electrolyte is common practice, for instance Angell jellified a range of lithium salts using polypropylene oxide [20]. Very recently, Abbot developed a biodegradable composite with good mechanical properties based on a mixture of a DES and starch [21].

2. Experimental

All starting materials were used as delivered and all work was performed under ambient conditions. The DES was prepared as previously described [14]. Unless otherwise stated all measurements were performed at 50 °C.

2.1. Preparation of separator

The jellified electrolyte was prepared by adding 5 wt.% polyvinyl alcohol (PVA, Mowiol 4-98, Mw ~27,000) to plain ethaline. The suspension of PVA flakes was heated in a covered beaker to 150 °C on a hotplate with stirring. After 90 min all the PVA dissolved to form a clear, colourless liquid. Upon cooling, a translucent gel is formed, which can be returned to the liquid state an indefinite number of times by reheating briefly to 150 °C. The composite separators used in this work were prepared by applying the hot liquid sequentially to both sides of a vertically suspended filter paper (Schleicher & Schuell, 589/1) and removing any excess using a flat spatula.

2.2. Description of redox flow battery

A simple RFB was constructed by sandwiching a separator between two polycarbonate plates. Sealing was achieved using silicone gaskets, which also served to hold a carbon cloth (E-tek elat GDL microporous layer on non-woven web, thin configuration) against each polycarbonate plate. Electrical connection to each cloth was made by compressing a short strip of platinum foil between the polycarbonate plate and the unwetted edge of the carbon cloth. The macroscopic area of exposed carbon cloth in each half cell was 5.5 cm^2, the separation between the composite separator and carbon cloth was 0.25 mm.

The two half-cell electrolytes were stored in two separate glass reservoirs fitted with thermostatic jackets. Pumping was achieved using a peristaltic pump, at a rate of 44 ml/min. The electrolyte from each half cell was returned to the same reservoir from which it originated.

The electrolyte used in the RFB was prepared by dissolving anhydrous $CuCl_2$ (Riedel de Häen, purum) in the DES at 50 °C in a closed vessel with stirring to form a 1 M solution. A length of single-strand copper wire (99.9% ASTM designation C100140) was introduced and the electrolyte left stirring for 12 h at 50 °C to allow the comproportionation reaction to occur. During comproportionation Cu(II) in solution oxidises Cu^0 to form Cu(I), Cu(II) is reduced to Cu(I) in the process. The solution still had a dark brown colour after the comproportionation reaction was stopped, at which point the copper wire was removed. Exposure of the freshly comproportionated solution to ambient conditions rapidly leads to the development of a green colour, which we speculate is due to the formation of a Cu(I) complex with oxygen.

2.3. Description of miniature redox battery

To determine the performance of the battery with minimal oxygen present and a well-defined, uniform cell temperature a battery was constructed using a pair of thermostated diffusion cells (PermeGear Horizontal Cell (Side-Bi-Side) 5G-00-00-09, chamber volume 2.4 ml). In the negative half-cell the electrolyte was plain ethaline and the electrode was a copper wire (99.9% ASTM designation C100140, diameter 0.5 mm, wound in a 3 mm spiral, effective electrode area of 3 cm^2). In the positive half-cell the electrolyte was a 0.5 M solution of anhydrous $CuCl_2$ (Riedel de Häen, purum) in ethaline and the electrode was a platinum wire (diameter 1 mm, wound in a 3 mm spiral, effective electrode area of 1.7 cm^2).

The distance between the two electrodes was 35 mm. The same separator used in the preparation of the RFB was used to prevent mixing of the two electrolytes, the diameter of the opening connecting the two cells was 9 mm, resulting in 0.636 cm^2 of the separator being available for ionic transport.

Since mass transport limitations at the electrodes appear to be the major limiting factor in this system, the two electrodes were purposefully dimensioned to give a geometric area in excess of the separator area. This provides a closer approximation to a typical RFB, which would utilise high surface area porous electrodes. Contamination of the electrolytes during operation was minimised by passing the electrodes through plastic stoppers, which minimised contact of the electrolytes with air. Only the electrolyte initially present at the time of loading the cells is available for conversion

during cycling. Convection in each half-cell is maintained using a pair of 7.5 mm magnetic stirrers.

2.4. Characterisation of the Cu(II)/Cu(I) reaction on glassy carbon and graphite using the RDE

The glassy carbon (GC) rotating disc electrode (RDE) was supplied by Pine Instruments (AFE3T050GC) and was prepared as previously described [18]. The graphite RDE was machined from graphite rod (Alfa Aesar 99.9995%), fitted in a Pine Instruments ChangeDisk tip assembly (AFE6R1PT) and polished using standard note paper.

The redox behaviour of the Cu(I)/Cu(II) chloro complexes were investigated at the GC electrode using a 20 mM $CuCl_2$ electrolyte prepared using anhydrous $CuCl_2$ (Riedel de Häen, purum). Measurements on the graphite electrode using this electrolyte were complicated by a slow background process, which may be related to the porous nature of the electrode. For this reason the kinetics at the graphite electrode were studied using the same 2 M Cu(I) electrolyte used for the RFB measurements.

100% IR correction was applied during RDE measurements. Steady-state voltammetry measurements were acquired using a staircase waveform. Provided the step size is sufficiently large this allows full relaxation of the Nernst diffusion layer at higher scan rates than are possible with cyclic voltammetry. This can be a matter of concern in viscous liquids at slow rotation speeds, if accurate determination of the heterogeneous kinetics is the objective. Relaxation of the Nernst layer was checked by performing the voltammetric measurements in both scan directions and validating that the current observed at each potential was independent of the scan direction.

Measurements performed using the RDE were analysed by preparing Koutecký-Levich plots to determine the kinetic current, I_k, at each potential. This was then used to quantify the heterogeneous rate constant, k^0, by preparing the Tafel plot. This method is described in detail in standard electrochemistry textbooks [22].

2.5. Instrumentation and electrochemical techniques

Measurements were performed using a Solartron 1286 potentiostat. Waveform generation and acquisition was performed using a National instruments 6251 DAQ controlled with custom Matlab software. All electrochemical measurements were preceded by measuring electrochemical impedance spectra (eis) at the open circuit potential (ocp) between 100 kHz. and 1 Hz. The intercept with the real axis in the complex plane plot was taken as the solution resistance.

The conductivity of ethaline was determined using a DC method we have previously reported [18]. The conductivity of jellified ethaline was determined by eis measurements of a gel that had been cast in a PTFE cylinder, of known geometry, which was sandwiched between two thermostated aluminium electrodes. The conductivity of the separator was determined in a similar manner, by sandwiching a sample between two copper discs inside the PTFE cylinder.

3. Results and discussion

3.1. Composition of electrolytes

The distribution of Cu(II) and Cu(I) species in the comproportionated electrolyte was estimated based on the cathodic and anodic limiting currents, $i_{l,c}$ and $i_{l,a}$, respectively, observed during staircase voltammetry measurements at an RDE, as shown in Fig. 1. These show that a portion of the Cu(II) remains unreacted. The

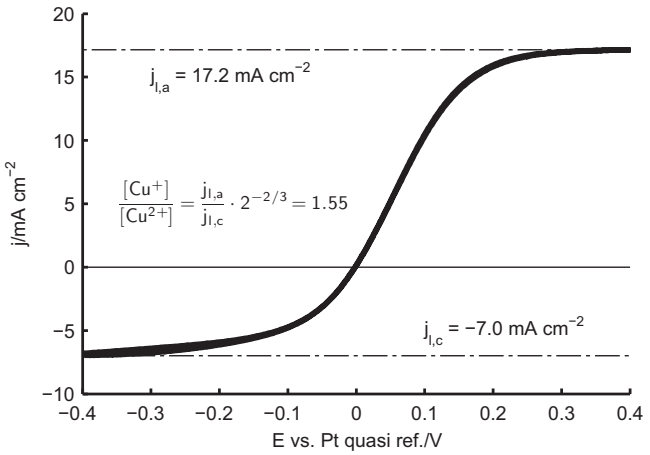

Fig. 1. Staircase voltammogram of a freshly comproportionated electrolyte measured at a GC RDE, prepared as described in Section 2.4. The $CuCl_2$ concentration was 1 M prior to introduction of the copper wire. The voltammogram was measured at 30 °C and at a rotation speed of 2000 rpm.

Levich equation indicates that for each of the two soluble electroactive species the resulting limiting current is proportional to the bulk concentration and the diffusion coefficient raised to the power of two-thirds. As we have previously reported, the diffusion coefficient of Cu(I) is twice that of Cu(II) [14]. Hence we can estimate the ratio of the bulk concentrations from the ratio of the limiting currents. Typically the concentration of Cu(II) complex in the comproportionated electrolyte is two-thirds of the Cu(I) complex concentration.

The comproportionated electrolyte has a strong green colour, which becomes faint yellow when diluted to concentrations suitable for UV–vis spectroscopy (~2 mM). UV–vis spectroscopy showed the presence of the same Cu(II) and Cu(I) species we have previously reported [14]. The identity of the high concentration species is not yet known. We have observed the same transition from a colourless complex when the comproportionation reaction is performed under argon to a green complex under ambient conditions for a chloride rich Cu(I) electrolyte based on 1-butyl-1-methylpyrrolidinium bis(trifluoromethylsulfonyl)imide [23].

During charge cycling of the miniature redox battery no green complex was observed at any point during operation. However, when the experiment was completed and the cell decommissioned the Cu(I) rich electrolyte from the negative half-cell was exposed to ambient conditions and also underwent a rapid transition from a colourless to a green complex.

3.2. Durability and permeability of the jellified membrane

Testing of the jellified membrane showed only minor permeation of the Cu(II) complex at 50 °C. During prolonged RFB testing at 50 °C, over periods of weeks, the jellified membranes maintained effective separation of the two electrolytes. The long term stability has not yet been proven. Since the battery chemistry reported here utilises only one element, permeation of the electroactive species through the membrane only impacts on the Coulombic efficiency of the system and should not cause a deterioration in long term performance.

3.3. Conductivity of the plain, gellified and supported electrolyte

Fig. 2 shows that the plain and jellified electrolyte have virtually indistinguishable conductivity over a range of temperatures. The conductivity of the composite separator, also shown in Fig. 2, is around four times lower than the plain electrolyte or gel. As the

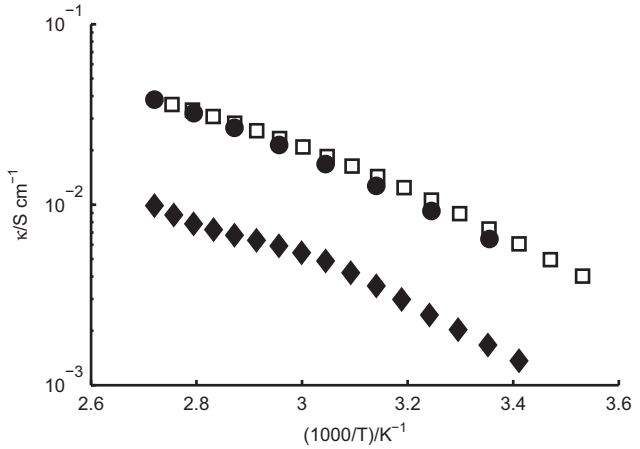

Fig. 2. Temperature dependence of conductivity for pure ethaline (□), ethaline gel containing 5 wt.% PVA (●) and ethaline gel supported in a filter paper (◊).

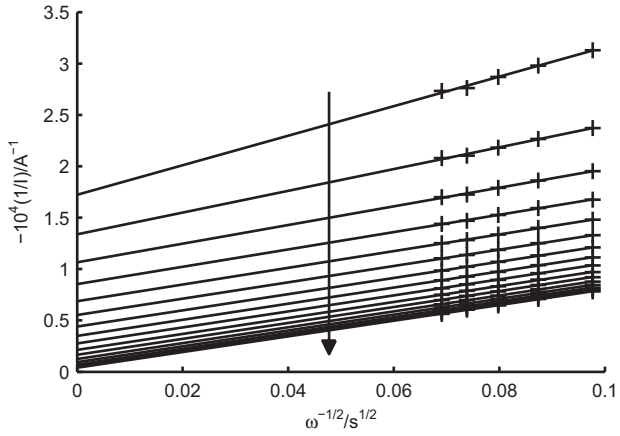

Fig. 4. Koutecký-Levich plots prepared from the voltammetric data shown in Fig. 3 for η values between −0.05 and −0.4 V. The arrow indicates increasingly negative overpotentials.

thickness of the composite separator is 300 μm it should contribute 30% of the ohmic losses in the RFB reported here. The conductivity of the gel prepared here is around three orders of magnitude higher than the DES-starch composite reported by Abbott [21].

3.4. Characterisation of the Cu(I)/Cu(II) redox reaction at a carbon electrodes

The reaction shown in Eq. (2) was characterised at glassy carbon and graphite rotating disc electrodes at rotation speeds of 1000, 1250, 1500, 1750 and 2000 rpm. Normalised voltammetry data for the glassy carbon electrode is shown in Fig. 3. This data was used to determine the kinetic current, I_k, at each potential by evaluation of the Koutecký-Levich equation. Fig. 4 shows this for the cathodic branch of the voltammetric data in Fig. 3. The resulting Tafel plots are shown in Fig. 5. By extrapolating the linear part of the cathodic branch of I_k to zero overpotential ($\eta = 0$) the exchange current, I_0, can be determined and this can be used to estimate k^0. On GC and graphite k^0 is 1.5×10^{-4} and 9.5×10^{-4} cm s^{-1}, respectively, compared to a value of 30×10^{-4} cm s^{-1} which we previously reported at a platinum electrode under the same conditions. These values appear favourable compared to the rate constant associated with the positive electrode reaction in conventional aqueous vanadium sulphate based RFBs, which is reported to be 2×10^{-6} cm s^{-1} [24].

The difference between glassy carbon and graphite may be attributable to the greater surface roughness of graphite, since I_0 was normalised by the macroscopic surface area to determine k^0. The higher rate on a platinum electrode may be attributable to mediation of the redox reaction by chloride ions adsorbed on the platinum surface, as has been reported in aqueous electrolytes [25].

3.5. Performance of an all copper RFB

Fig. 6 shows the staircase voltammogram of the all copper RFB described in Section 2.2 after two weeks operation under ambient conditions. The transition from charging to discharging occurs at 0.72 V, which is indicative of the expected cell potential. The window of stability of the electrolyte was 2.5 V when using graphite electrodes. The ohmic impedance of the RFB was 20.7 Ωcm^2, which is around four times higher than would be expected based on the conductivity results shown in Fig. 2 and may indicate either additional ohmic losses, for instance in the carbon cloth, or poor control of temperature. After running a deposition cycle at limiting current for 2 h the RFB was opened and the copper deposit on the negative electrode was found to be matte, adherent and free of dendrites.

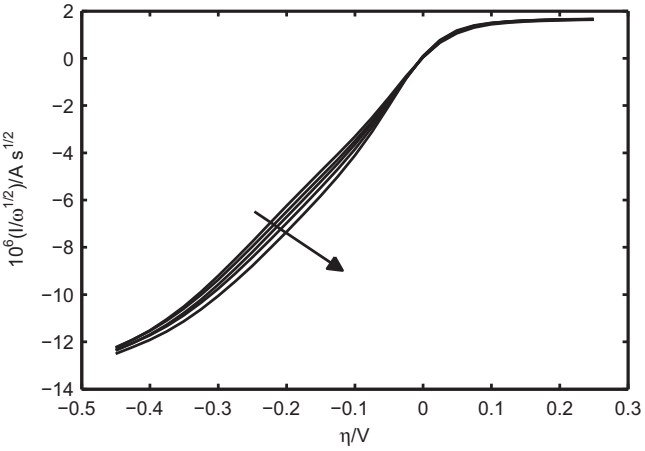

Fig. 3. Normalised staircase voltammetry data for a 20 mM $CuCl_2$ electrolyte at a 5 mm GC electrode at rotation rates of 1000, 1250, 1500, 1750 and 2000 rpm. The arrow indicates decreasing rotation speed. 100% IR correction was applied during acquisition of the voltammogram.

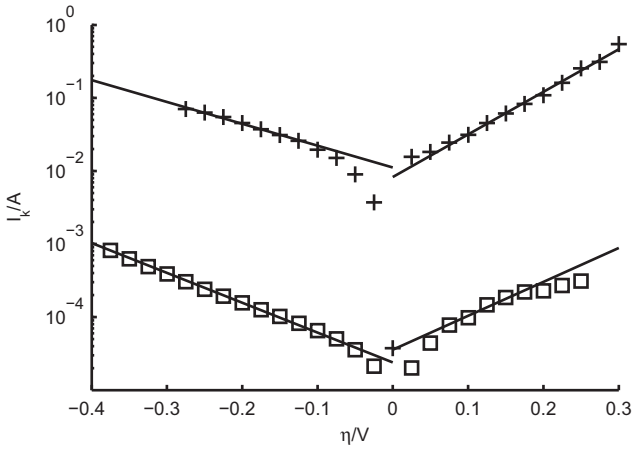

Fig. 5. Tafel plot for a 20 mM $CuCl_2$ electrolyte at a glassy carbon electrode (□) and a 2 M CuCl electrolyte at a graphite electrode (+) The I_k values for the GC electrode measured at negative η values are determined from the intercept of the Koutecký-Levich plots shown in Fig. 4.

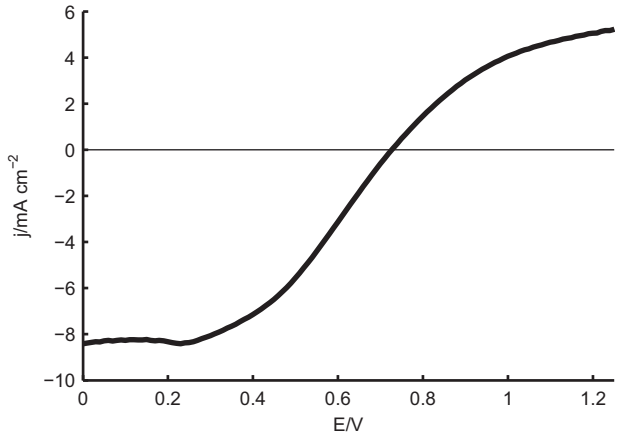

Fig. 6. Staircase voltammogram of the all copper RFB described in Section 2.2.

3.6. Performance of a miniature redox battery

The miniature redox battery described in Section 2.3 was also used to check the applicability of the ex-situ conductivity measurements. Based on the approximate geometry of the diffusion cells and ex situ conductivity measurements a total cell impedance of 318 Ohm was expected at 50 °C, of which 9 Ohm would be attributable to the separator. In practise, measurements with this battery in the presence and absence of a separator showed impedances of 267 Ohm and 256 Ohm, respectively, with some of the 20% difference from the ex-situ measurements possibly being attributable to the slightly larger aperture of the cell in the vicinity of the stirrer. This proves that the ex situ conductivity measurements can provide a good indication of the performance that can be expected in a complete cell, provided all other ohmic losses are minimised and the temperature is well defined. It also demonstrates that the conductivity of the electrolyte is largely unchanged at the solute concentrations used in this work and still corresponds to that of ethaline.

The long-term performance of the redox chemistry presented in this work was tested by performing charge cycling in the miniature redox battery over a period of seven days. A current density of 10 mA/cm^2 (normalised used the separator area) was used for this operation. During this time the battery was cycled 38 times. The coulombic and energy efficiencies, η_Q and η_E, respectively, showed little deviation over time, averaging 94.3±6.6% and 52.1±9.1% respectively.

During charging and discharging the typical amount of charge passed were $Q_{charge} = 23.0 \pm 4.6$ and $Q_{discharge} = -21.8 \pm 5.5$ C respectively. This corresponds to only a fifth of the theoretical capacity, Q_{theory} of the battery based on the amount of $CuCl_2$ used. The variation in η_Q, η_E and Q_{charge} over time is shown in Fig. 7.

The ocp values measured after each charge or discharge operation were equally invariant over the time of operation with values of 0.773 ± 0.006 and 0.683 ± 0.004 V respectively. These potentials agree well with the voltammetric data for the higher concentration electrolyte shown in Fig. 6.

Fig. 8 shows charge–discharge cycles 24–27. These were performed at a lower current density of 7.5 mA/cm^2, this appeared to benefit the performance of the battery significantly, resulting in a doubling of the amount of current passed to 46.8 ± 2 C, which corresponds to a 40% depletion of the theoretical battery capacity. Energy efficiency also improved, with an average value of 62 ± 1%. The coulombic efficiency was unchanged. Ocp values after charging and discharging shifted to 0.806 ± 0.006 V and 0.672 ± 0.002 V, respectively, with the larger shift in the ocp after charging explaining some of the increase in efficiency.

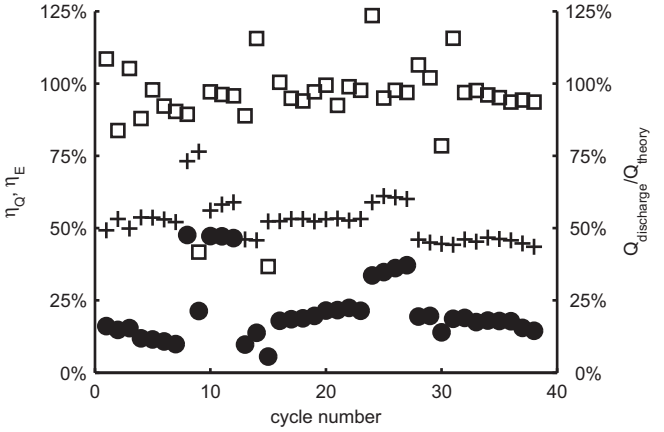

Fig. 7. The evolution of Coulombic efficiency, η_Q (□), energy efficiency, η_E (+), and the discharge capacity, $Q_{discharge}$ (●), normalised by the theoretical capacity, Q_{theory}, during 38 charge–discharge cycles for the redox battery described in Section 2.3. Cycling was performed at a current density of 10 mA/cm^2, with the exception of cycles 8–9 and 24–27 which were performed at current densities of 4 and 7.5 mA/cm^2 respectively. The pronounced outliers in η_Q correlate with changes in the applied current density and resolve within a few cycles.

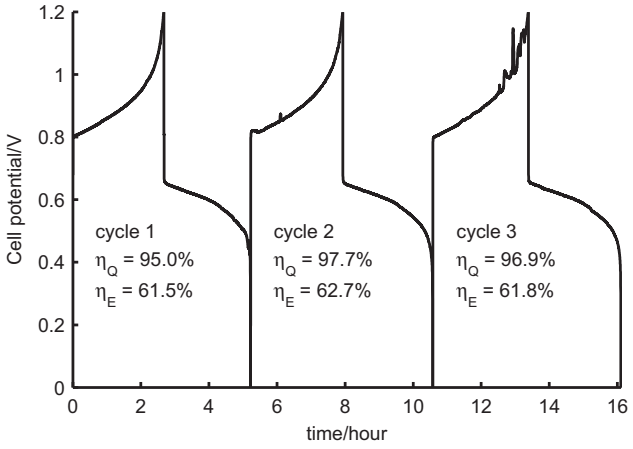

Fig. 8. Three charge/discharge cycles performed in the miniature redox battery described in Section 2.3 at a current density of 7.5 mA/cm^2, post experimental correction of the ohmic losses in the cell were applied as described previously [18].

Charge–discharge cycles 8 and 9 of Fig. 7 were performed at a current density of only 4 mA/cm^2. This appears to improve energy efficiency further, with both cycles displaying an energy efficiency of around 75%. However, since a single charge–discharge cycle required 14 h this current density was not used for further measurements and hence insufficient cycles were acquired to validate the reproducibility of the observed energy efficiency.

4. Conclusions

The redox reactions selected exhibit reasonable electrochemical kinetics. However, the small ocp suggests an all copper RFB is not a useful battery system, particularly in poorly conductive electrolytes such as ILs where ohmic losses are pronounced.

An appreciable current density was not achievable in the RFB, despite the high metal concentration in solution, due to the poor mass transport properties of the electrolyte. Even had a current density of, for example, 50 mA/cm^2 been achieved, this would have resulted in ohmic losses of around 0.5 V and negligible efficiency. Elevating the operating temperature will reduce this problem and should be possible based on the separator presented here.

This work has demonstrated that conceptually a DES based electrolyte system can be employed in a RFB and shown the simple preparation of a suitable separator. None of the problems associated with chlorocuprate electrolytes reported by Porterfield and Yoke [19] were apparent, provided the electrolyte temperature was kept at 50 °C or higher, suggesting that DES are suited for further investigation as RFB electrolyte media. The behaviour of the system, for instance the conductivity, cell potentials and electrode kinetics, showed good reproducibility across the range of concentrations reported here. We will explore this further utilising an improved stack design that facilitates higher temperatures and alternative redox couples that allow larger cell potentials.

For ethaline the viscosity, conductivity and speciation of metal complexes are similar to chloride rich ionic liquids, while the ease of handling and cost are improved. This makes it, at the very least, a useful platform to develop the application of ILs as electrolyte media for RFBs. In this work we have shown the preparation of a simple separator which should be widely applicable for a range of ionic liquids. Due to the small electrolyte volumes, excellent temperature control, corrosion resistance and relative simplicity, the miniature redox battery reported here is also particularly suitable for initial measurements of novel redox systems in ionic liquids or molten salts.

References

[1] M. Skyllas-Kazacos, M.H. Chakrabarti, S.A. Hajimolana, F.S. Mjalli, M. Saleem, Progress in flow battery research and development, Journal of The Electrochemical Society 158 (2011) R55.

[2] C. Wadia, P. Albertus, V. Srinivasan, Resource constraints on the battery energy storage potential for grid and transportation applications, Journal of Power Sources 196 (2011) 1593.

[3] G. Nikiforidis, L. Berlouis, D. Hall, D. Hodgson, Evaluation of carbon composite materials for the negative electrode in the zinc-cerium redox flow cell, Journal of Power Sources 206 (2012) 497.

[4] T. Tsuda, C.L. Hussey, electrochemistry of room-temperature ionic liquids and melts Modern Aspects of Electrochemistry, vol. 45, Springer, New York, 2009.

[5] M. Lipsztajn, R.A. Osteryoung, Electrochemistry in neutral ambient-temperature ionic liquids. 1. Studies of iron(III), neodymium(III), and lithium(I), Inorganic Chemistry 24 (1985) 716.

[6] H.D. Pratt III, A.J. Rose, C.L. Staiger, D. Ingersoll, T.M. Anderson, Synthesis and characterization of ionic liquids containing copper, manganese, or zinc coordination cations, Dalton Transactions 40 (2011) 11396.

[7] C. Austen Angell, Y. Ansari, Z. Zhao, Ionic liquids: past, present and future, Faraday Discussions 154 (2012) 9.

[8] T. Katase, K. Murase, T. Hirato, Y. Awakura, Redox and transport behaviors of Cu(I) ions in TMHA-Tf2N ionic liquid solution, Journal of Applied Electrochemistry 37 (2007) 339.

[9] T.M. Anderson, D. Ingersoll, A.J. Rose, C.L. Staiger, J.C. Leonard, Synthesis of an ionic liquid with an iron coordination cation, Dalton Transactions 39 (2010) 8609.

[10] D. Zhang, Q. Liu, X. Shi, Y. Li, Tetrabutylammonium hexafluorophosphate and 1-ethyl-3-methyl imidazolium hexafluorophosphate ionic liquids as supporting electrolytes for non-aqueous vanadium redox flow batteries, Journal of Power Sources 203 (2012) 201.

[11] R.L. Kay, B.J. Hales, G.P. Cunningham, Conductance and association behavior of the alkali metal perchlorates and tetraphenylborides in anhydrous acetonitrile, Journal of Physical Chemistry 71 (1967) 3925.

[12] A.P. Abbott, K.J. McKenzie, Application of ionic liquids to the electrodeposition of metals, Physical Chemistry Chemical Physics 8 (2006) 4265.

[13] A.P. Abbott, G. Frisch, K.S. Ryder, Metal complexation in ionic liquids, Annual Reports on the Progress of Chemistry, Section A: Inorganic Chemistry 104 (2008) 21.

[14] D. Lloyd, T. Vainikka, L. Murtomäki, K. Kontturi, E. Ahlberg, The kinetics of the Cu(II)/Cu(I) redox couple in deep eutectic solvents, Electrochimica Acta 56 (2011) 4942.

[15] A.P. Abbott, G. Capper, K.J. McKenzie, A. Glidle, K.S. Ryder, Electropolishing of stainless steels in a choline chloride based ionic liquid: an electrochemical study with surface characterisation using sem and atomic force microscopy, Physical Chemistry Chemical Physics 8 (2006) 4214.

[16] A.P. Abbott, K. El Ttaib, G. Frisch, K.J. McKenzie, K.S. Ryder, Electrodeposition of copper composites from deep eutectic solvents based on choline chloride, Physical Chemistry Chemical Physics 11 (2009) 4269.

[17] K. Haerens, E. Matthijs, K. Binnemans, B. Van der Bruggen, Electrochemical decomposition of choline chloride based ionic liquid analogues, Green Chemistry 11 (2009) 1357.

[18] D. Lloyd, T. Vainikka, S. Schmachtel, L. Murtomäki, K. Kontturi, Simultaneous characterisation of electrode kinetics and electrolyte properties in ionic liquids using a rotating disc electrode, Electrochimica Acta 69 (2012) 139.

[19] W.W. Porterfield, J.T. Yoke, Inorganic Compounds with Unusual Properties, ACS Publications, Washington, DC, p. 104, 1976.

[20] C. Angell, C. Liu, E. Sanchez, Rubbery solid electrolytes with dominant cationic transport and high ambient conductivity, Nature (1993) 137.

[21] A.P. Abbott, A.D. Ballantyne, J.P. Conde, K.S. Ryder, W.R. Wise, Salt modified starch: sustainable, recyclable plastics, Green Chemistry 14 (2012) 1302.

[22] A. Bard, L. Faulkner, Electrochemical Methods: Fundamentals and Applications, Wiley, 2000.

[23] T. Vainikka, D. Lloyd, L. Murtomäki, J.A. Manzanares, K. Kontturi, Electrochemical study of copper chloride complexes in the RTIL 1-butyl-1-methylpyrrolidinium bis(trifluoromethylsulfonyl)imide, Electrochimica Acta 87 (2013) 739.

[24] A.Z. Weber, M.M. Mench, J.P. Meyers, P.N. Ross, J.T. Gostick, Q. Liu, Redox flow batteries: a review, Journal of Applied Electrochemistry 41 (2011) 1137.

[25] N.G. Hung, Z. Nagy, Kinetics of the ferrous/ferric electrode reaction in the absence of chloride catalysis, Journal of the Electrochemical Society 134 (1987) 2215.